Proposed Macroscopic Test of the Physical Relevance of Bell's Theorem

Joy Christian*
Einstein Centre for Local-Realistic Physics, 15 Thackley End, Oxford OX2 6LB, United Kingdom

A macroscopic experiment capable of detecting a signature of spinorial sign changes is discussed. If realized, it would determine whether Bell inequalities are satisfied for a manifestly local, classical system. By providing an explicitly local-realistic derivation of the EPR-Bohm type spin correlations, it is demonstrated why Bell inequalities must be violated even in such a manifestly local, macroscopic domain, just as strongly as they are in the microscopic domain. The proposed experiment has the potential to transform our understanding of the relationship between classical and quantum physics.

In a recent paper we have proposed a mechanical experiment to test possible macroscopic observability of spinorial sign changes under 2π rotations [1]. The proposed experiment is a variant of the local model for the spin-1/2 particles considered by Bell [2], which was later further developed by Peres providing pedagogical details [3][4]. Our experiment differs, however, from the one considered by Bell and Peres in one important respect. It involves measurements of the actual spin angular momenta of two fragments of an exploding bomb rather than their normalized spin values, ± 1. The latter are to be computed only after all runs of the experiment are completed, which can be executed either in the outer space or in a terrestrial laboratory. In the latter case the effects of gravity and air resistance may complicate matters, but it may be possible to choose experimental parameters sufficiently carefully to compensate for such effects.

With this assumption, consider a "bomb" made out of a hollow toy ball of diameter, say, three centimeters. The thin hemispherical shells of uniform density that make up the ball are snapped together at their rims in such a manner that a slight increase in temperature would pop the ball open into its two constituents with considerable force. A small lump of density much greater than the density of the ball is attached on the inner surface of each shell at a random location, so that, when the ball pops open, not only would the two shells propagate with equal and opposite linear momenta orthogonal to their common plane, but would also rotate with equal and opposite spin momenta about a random axis in space (see Fig. 1). The volume of the attached lumps can be as small as a cubic millimeter, whereas their mass can be comparable to the mass of the ball. This will facilitate some 10^6 possible spin directions for the two shells, whose outer surfaces can be decorated with colors to make their rotations easily detectable [1].

Now consider a large ensemble of such balls, identical in every respect except for the relative locations of the two lumps (affixed randomly on the inner surface of each shell). The balls are then placed over a heater—one at a time—at the center of the experimental setup [3], with the common plane of their shells held perpendicular to the horizontal direction of the setup. Although initially at rest, a slight increase in temperature of each ball will eventually eject its two shells towards the observation stations, situated at a chosen distance in the mutually opposite directions. Instead of selecting the directions $\mathbf{a}$ and $\mathbf{b}$ for observing spin components, however, one or more contact-less rotational motion sensors—capable of determining the precise direction of rotation—are placed near each of the two stations, interfaced with a computer (an improved setup and further practical details are discussed below). These sensors will determine the exact direction of the spin angular momentum $\mathbf{s}^k$ (or $-\,\mathbf{s}^k$) for each shell in a given explosion, without disturbing them otherwise so that their total angular momentum would remain zero, at a designated distance from the center. The interfaced computers can then record this data, in the form of a 3D map of all such directions, at each station.

Once the actual directions of the angular momenta for a large ensemble of shells on both sides are fully recorded, the two computers are instructed to choose a pair of reference directions, $\mathbf{a}$ for one station and $\mathbf{b}$ for the other station—from the two 3D maps of already existing data—and then calculate the corresponding pair of numbers $sign\,(+\,\mathbf{s}_1^k\cdot\mathbf{a}) = \pm\,1$ and $sign\,(-\,\mathbf{s}_2^k\cdot\mathbf{b}) = \pm\,1$. The standard correlation function for the two bomb fragments can then be calculated as

$$\mathcal{E}(\mathbf{a},\,\mathbf{b}) = \lim_{n\,\gg\,1}\left[\frac{1}{n}\sum_{k\,=\,1}^{n}\{sign\,(+\,\mathbf{s}_1^k\cdot\mathbf{a})\}\,\{sign\,(-\,\mathbf{s}_2^k\cdot\mathbf{b})\}\right], \tag{1}$$

together with

$$\mathcal{E}(\mathbf{a}) = \lim_{n\,\gg\,1}\left[\frac{1}{n}\sum_{k\,=\,1}^{n}\{sign\,(+\,\mathbf{s}_1^k\cdot\mathbf{a})\}\right] \,=\, 0 \,=\, \lim_{n\,\gg\,1}\left[\frac{1}{n}\sum_{k\,=\,1}^{n}\{sign\,(-\,\mathbf{s}_2^k\cdot\mathbf{b})\}\right] = \mathcal{E}(\mathbf{b})\,, \tag{2}$$

*Electronic address: jjc@alum.bu.edu

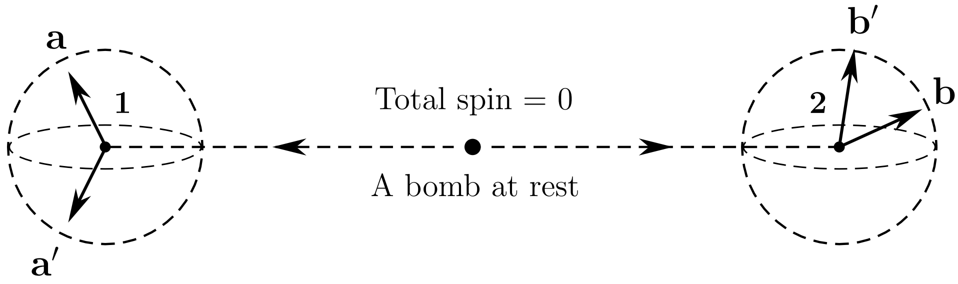

FIG. 1: A bomb, initially at rest, explodes into two unequal fragments carrying opposite spin angular momenta. Measurements of the spin components on each fragment are performed at remote stations **1** and **2**, along two post-selected directions **a** and **b**.

where n is the total number of experiments performed. A naïve computation of Eq. (1) by Bell [2] and Peres [3] gives

$$\mathcal{E}(\mathbf{a},\,\mathbf{b})\,=\begin{cases}-1\,+\,\frac{2}{\pi}\,\cos^{-1}(\mathbf{a}\cdot\mathbf{b}) & \text{if}\quad 0\leq\cos^{-1}(\mathbf{a}\cdot\mathbf{b})\leq\pi\\ \\ +3\,-\,\frac{2}{\pi}\,\cos^{-1}(\mathbf{a}\cdot\mathbf{b}) & \text{if}\quad \pi\leq\cos^{-1}(\mathbf{a}\cdot\mathbf{b})\leq 2\pi\,.\end{cases}\tag{3}$$

In what follows we shall compute the correlation function (1) correctly by taking into account the correct geometry and topology of the physical space [1]. This amounts to modeling the physical space by a quaternionic 3-sphere rather than by a flat Euclidean 3-space. Evidently, in the above experiment the two macroscopic bomb fragments would be rotating in tandem, *relative* to each other. Consequently, the observables $sign\,(+\,\mathbf{s}_1^k\cdot\mathbf{a})$ and $sign\,(-\,\mathbf{s}_2^k\cdot\mathbf{b})$ should be sensitive to the *relative* spinorial sign changes between these fragments. The correlation function (1) should then provide a measure of such sign changes in terms of the geodesic distance on the manifold SU(2) $\sim S^3$, which can be thought of as the configuration space of all possible rotations of the bomb fragment, including spinorial sign changes:

$$S^3:=\left\{\mathbf{q}(\psi,\,\mathbf{n}):=\exp\left[\boldsymbol{\beta}(\mathbf{n})\,\frac{\psi}{2}\right]\,\middle|\;||\,\mathbf{q}(\psi,\,\mathbf{n})\,||^2=1\right\},\tag{4}$$

where $\boldsymbol{\beta}(\mathbf{n})$ is a bivector rotating about $\mathbf{n}\in\mathrm{I\!R}^3$ with the rotation angle ψ in the range $0\leq\psi<4\pi$. Throughout this paper and elsewhere we have followed the notations, conventions, and terminology of geometric algebra [5][1]. Accordingly, the bivector $\boldsymbol{\beta}(\mathbf{n})\in S^2\subset S^3$ can be parameterized by a unit vector $\mathbf{n}=n_x\,\mathbf{e}_x+n_y\,\mathbf{e}_y+n_z\,\mathbf{e}_z\in\mathrm{I\!R}^3$ as

$$\boldsymbol{\beta}(\mathbf{n})\,:=\,(\,I\cdot\mathbf{n}\,)\,=\,n_x\,(\,I\cdot\mathbf{e}_x\,)\,+\,n_y\,(\,I\cdot\mathbf{e}_y\,)\,+\,n_z\,(\,I\cdot\mathbf{e}_z\,)\,=\,n_x\,\mathbf{e}_y\,\wedge\,\mathbf{e}_z\,+\,n_y\,\mathbf{e}_z\,\wedge\,\mathbf{e}_x\,+\,n_z\,\mathbf{e}_x\,\wedge\,\mathbf{e}_y\,,\tag{5}$$

with $\boldsymbol{\beta}^2(\mathbf{n})=-1$. Here the trivector $I:=\mathbf{e}_x\,\wedge\,\mathbf{e}_y\,\wedge\,\mathbf{e}_z$ (which also squares to -1) represents a volume form of the physical space [5][1]. Each configuration of the rotating fragment can thus be represented by a quaternion of the form

$$\mathbf{q}(\psi,\,\mathbf{n})\,=\,\cos\frac{\psi}{2}\,+\,\boldsymbol{\beta}(\mathbf{n})\,\sin\frac{\psi}{2}\,,\tag{6}$$

which in turn can always be decomposed into a product of two bivectors, say $\boldsymbol{\beta}(\mathbf{u})$ and $\boldsymbol{\beta}(\mathbf{v})$, belonging to an $S^2\subset S^3$,

$$\boldsymbol{\beta}(\mathbf{u})\,\boldsymbol{\beta}(\mathbf{v})\,=\,\cos\frac{\psi}{2}\,+\,\boldsymbol{\beta}(\mathbf{n})\,\sin\frac{\psi}{2}\,,\tag{7}$$

with ψ being its rotation angle from $\mathbf{q}(0,\,\mathbf{n})=1$. Note also that $\mathbf{q}(\psi,\,\mathbf{n})$ reduces to $\pm\,1$ as $\psi\rightarrow\,2\kappa\pi$ for $\kappa\,=\,0,\,1,$ or $2.$ More significantly for our purposes here, it is easy to verify that $\mathbf{q}(\psi,\,\mathbf{n})$ respects the following rotational symmetries:

$$\mathbf{q}(\psi+2\kappa\pi,\,\mathbf{n})\,=\,-\,\mathbf{q}(\psi,\,\mathbf{n})\quad\text{for}\;\;\kappa=1,3,5,7,\dots\tag{8}$$

$$\mathbf{q}(\psi+4\kappa\pi,\,\mathbf{n})\,=\,+\,\mathbf{q}(\psi,\,\mathbf{n})\quad\text{for}\;\;\kappa=0,1,2,3,\dots\tag{9}$$

Thus $\mathbf{q}(\psi,\,\mathbf{n})$ correctly represents the state of fragment that returns to itself only after even multiples of a 2π rotation.

It is also worth recalling here that, on the physical grounds, angular momenta are in general best represented, not by ordinary polar vectors, but by pseudo-vectors, or bivectors, that change sign upon reflection [1]. One only has to compare a spinning object, like a barber's pole, with its image in a mirror to appreciate this elementary fact. The mirror image of a polar vector representing the spinning object is not the polar vector that represents the mirror image of the spinning object. In fact it is the negative of the polar vector that does the job. Therefore the spin angular momenta of the two bomb fragments considered above are better represented by a set of unit bivectors using the powerful language of geometric algebra [5]. They can be expressed in terms of graded bivector bases with sub-algebra

$$L_\mu(\lambda)\,L_\nu(\lambda)\;=\;-\,\delta_{\mu\nu}\;-\;\sum_\rho \epsilon_{\mu\nu\rho}\,L_\rho(\lambda)\,, \tag{10}$$

which span a tangent space at each point of S^3, with a choice of orientation $\lambda = \pm\,1$ [1]. Contracting this equation on both sides with the components a^μ and b^ν of arbitrary unit vectors $\mathbf{a}$ and $\mathbf{b}$ then gives the convenient bivector identity

$$\mathbf{L}(\mathbf{a},\,\lambda)\,\mathbf{L}(\mathbf{b},\,\lambda)\;=\;-\,\mathbf{a}\cdot\mathbf{b}\;-\;\mathbf{L}(\mathbf{a}\times\mathbf{b},\,\lambda)\,, \tag{11}$$

which is simply a geometric product between the unit bivectors representing the spin momenta considered previously:

$$\mathbf{L}(\mathbf{a},\,\lambda)\;=\;\lambda\,I\,\mathbf{a}\;=\;\lambda\,I\cdot\mathbf{a}\;\equiv\;\lambda(\mathbf{e}_x\wedge\mathbf{e}_y\wedge\mathbf{e}_z)\cdot\mathbf{a}\;=\;\pm 1\text{ spin about the direction }\mathbf{a} \tag{12}$$

$$\text{and}\quad \mathbf{L}(\mathbf{b},\,\lambda)\;=\;\lambda\,I\,\mathbf{b}\;=\;\lambda\,I\cdot\mathbf{b}\;\equiv\;\lambda(\mathbf{e}_x\wedge\mathbf{e}_y\wedge\mathbf{e}_z)\cdot\mathbf{b}\;=\;\pm 1\text{ spin about the direction }\mathbf{b}\,, \tag{13}$$

where the trivector $I := \mathbf{e}_x\wedge\mathbf{e}_y\wedge\mathbf{e}_z$ with $I^2 = -1$ represents the volume form on S^3 and ensures that $\mathbf{L}^2(\mathbf{n},\,\lambda) = -1$.

We are now in a position to derive the correlation between the spins in a succinct and elegant manner. To this end, let us pretend that the emerging spin bivectors $\mp\,\mathbf{L}(\mathbf{s},\,\lambda^k)$ are detected by detector bivectors $\mathbf{D}(\mathbf{a})$ and $\mathbf{D}(\mathbf{b})$, giving

$$S^3 \ni sign(+\,\mathbf{s}_1^k\cdot\mathbf{a}) \;:=\; \lim_{\mathbf{s}_1\,\to\,\mathbf{a}}\left\{-\,\mathbf{D}(\mathbf{a})\,\mathbf{L}(\mathbf{s}_1,\,\lambda^k)\right\} = \begin{Bmatrix} +1 & \text{if} & \lambda^k\;=\;+\,1 \\ -\,1 & \text{if} & \lambda^k\;=\;-\,1 \end{Bmatrix} \text{ with } \Big\langle\, sign(+\,\mathbf{s}_1^k\cdot\mathbf{a})\,\Big\rangle \;=\; 0 \tag{14}$$

$$\text{and}\quad S^3 \ni sign(-\,\mathbf{s}_2^k\cdot\mathbf{b}) \;:=\; \lim_{\mathbf{s}_2\,\to\,\mathbf{b}}\left\{+\,\mathbf{L}(\mathbf{s}_2,\,\lambda^k)\,\mathbf{D}(\mathbf{b})\right\} = \begin{Bmatrix} -\,1 & \text{if} & \lambda^k\;=\;+\,1 \\ +1 & \text{if} & \lambda^k\;=\;-\,1 \end{Bmatrix} \text{ with } \Big\langle\, sign(-\,\mathbf{s}_2^k\cdot\mathbf{b})\,\Big\rangle \;=\; 0\,, \tag{15}$$

where we assume the orientation λ of S^3 to be a random variable with 50/50 chance of being $+1$ or $-\,1$ at the moment of bomb explosion, making the spinning bivector $\mathbf{L}(\mathbf{n},\,\lambda^k)$ a random variable *relative* to the detector bivector $\mathbf{D}(\mathbf{n})$:

$$\mathbf{L}(\mathbf{n},\,\lambda^k)\;=\;\lambda^k\,\mathbf{D}(\mathbf{n})\;\Longleftrightarrow\;\mathbf{D}(\mathbf{n})\;=\;\lambda^k\,\mathbf{L}(\mathbf{n},\,\lambda^k)\,. \tag{16}$$

Note that LHS and RHS of Eqs. (14) and (15) describe, respectively, one and the same scalar point of the 3-sphere, albeit with different algebraic expressions. To see this more explicitly, we can expand the RHS of Eq. (14) as follows:

$$\lim_{\mathbf{s}_1\,\to\,\mathbf{a}}\left\{-\,\mathbf{D}(\mathbf{a})\,\mathbf{L}(\mathbf{s}_1,\,\lambda^k)\right\} \;=\; \lim_{\mathbf{s}_1\,\to\,\mathbf{a}}\left\{-\,\lambda^k\,\mathbf{L}(\mathbf{a},\,\lambda^k)\,\mathbf{L}(\mathbf{s}_1,\,\lambda^k)\right\} \tag{17}$$

$$=\;\lim_{\mathbf{s}_1\,\to\,\mathbf{a}}\left[-\lambda^k\left\{-\,\mathbf{a}\cdot\mathbf{s}_1\;-\;\mathbf{L}(\mathbf{a}\times\mathbf{s}_1,\,\lambda^k)\right\}\right] \tag{18}$$

$$=\;\lim_{\mathbf{s}_1\,\to\,\mathbf{a}}\left\{+\,\mathbf{a}\cdot(\lambda^k\,\mathbf{s}_1)\;+\;I\cdot(\mathbf{a}\times\mathbf{s}_1)\right\} \tag{19}$$

$$=\;sign(+\,\mathbf{s}_1^k\cdot\mathbf{a})\,,\;\;\text{with}\;\;\mathbf{s}_1^k\equiv\lambda^k\,\mathbf{s}_1, \tag{20}$$

where Eqs. (16), (11), and (12) are used. Likewise we can expand the RHS of Eq. (15) using Eqs. (16), (11), and (13):

$$\lim_{\mathbf{s}_2\,\to\,\mathbf{b}}\left\{+\,\mathbf{L}(\mathbf{s}_2,\,\lambda^k)\,\mathbf{D}(\mathbf{b})\right\} \;=\; \lim_{\mathbf{s}_2\,\to\,\mathbf{b}}\left\{+\,\mathbf{L}(\mathbf{s}_2,\,\lambda^k)\,\lambda^k\,\mathbf{L}(\mathbf{b},\,\lambda^k)\right\} \tag{21}$$

$$=\;\lim_{\mathbf{s}_2\,\to\,\mathbf{b}}\left[+\lambda^k\left\{-\,\mathbf{s}_2\cdot\mathbf{b}\;-\;\mathbf{L}(\mathbf{s}_2\times\mathbf{b},\,\lambda^k)\right\}\right] \tag{22}$$

$$=\;\lim_{\mathbf{s}_2\,\to\,\mathbf{b}}\left\{-\,(\lambda^k\,\mathbf{s}_2)\cdot\mathbf{b}\;-\;I\cdot(\mathbf{s}_2\times\mathbf{b})\right\} \tag{23}$$

$$=\;sign(-\,\mathbf{s}_2^k\cdot\mathbf{b})\,,\;\;\text{with}\;\;\mathbf{s}_2^k\equiv\lambda^k\,\mathbf{s}_2. \tag{24}$$

Moreover, as demanded by the conservation of angular momentum, we require the total spin to respect the condition

$$-\,\mathbf{L}(\mathbf{s}_1,\,\lambda^k)\;+\;\mathbf{L}(\mathbf{s}_2,\,\lambda^k)\;=\;0\quad\Longleftrightarrow\quad\mathbf{L}(\mathbf{s}_1,\,\lambda^k)\;=\;\mathbf{L}(\mathbf{s}_2,\,\lambda^k)\quad\Longleftrightarrow\quad\mathbf{s}_1\;=\;\mathbf{s}_2\;\equiv\;\mathbf{s}\quad[\text{cf. Fig. 1}]. \tag{25}$$

Evidently, in the light of the product rule (11) for the unit bivectors, the above condition is equivalent to the condition

$$\mathbf{L}(\mathbf{s}_1,\,\lambda^k)\,\mathbf{L}(\mathbf{s}_2,\,\lambda^k)\,=\,\big\{\,\mathbf{L}(\mathbf{s},\,\lambda^k)\big\}^2\,=\,\mathbf{L}^2(\mathbf{s},\,\lambda^k)\,=\,-1\,. \tag{26}$$

The average of simultaneous events $sign(+\,\mathbf{s}_1^k\cdot\mathbf{a})=\pm1$ and $sign(-\,\mathbf{s}_2^k\cdot\mathbf{b})=\pm1$ within S^3 then works out as follows:

$$\begin{aligned}
\mathcal{E}(\mathbf{a},\,\mathbf{b})\,&=\,\lim_{n\,\rightarrow\,\infty}\left[\frac{1}{n}\sum_{k\,=\,1}^{n}\,sign(+\,\mathbf{s}_1^k\cdot\mathbf{a})\;sign(-\,\mathbf{s}_2^k\cdot\mathbf{b})\right] &(27)\\
&=\,\lim_{n\,\rightarrow\,\infty}\left[\frac{1}{n}\sum_{k\,=\,1}^{n}\,\left[\lim_{\mathbf{s}_1\,\rightarrow\,\mathbf{a}}\big\{-\mathbf{D}(\mathbf{a})\,\mathbf{L}(\mathbf{s}_1,\,\lambda^k)\big\}\right]\left[\lim_{\mathbf{s}_2\,\rightarrow\,\mathbf{b}}\big\{+\mathbf{L}(\mathbf{s}_2,\,\lambda^k)\,\mathbf{D}(\mathbf{b})\big\}\right]\right] &(28)\\
&=\,\lim_{n\,\rightarrow\,\infty}\left[\frac{1}{n}\sum_{k\,=\,1}^{n}\,\lim_{\substack{\mathbf{s}_1\,\rightarrow\,\mathbf{a}\\ \mathbf{s}_2\,\rightarrow\,\mathbf{b}}}\big\{-\mathbf{D}(\mathbf{a})\,\big\}\,\big\{\,\mathbf{L}(\mathbf{s}_1,\,\lambda^k)\;\mathbf{L}(\mathbf{s}_2,\,\lambda^k)\,\big\}\,\big\{+\mathbf{D}(\mathbf{b})\,\big\}\right] &(29)\\
&=\,\lim_{n\,\rightarrow\,\infty}\left[\frac{1}{n}\sum_{k\,=\,1}^{n}\,\lim_{\substack{\mathbf{s}_1\,\rightarrow\,\mathbf{a}\\ \mathbf{s}_2\,\rightarrow\,\mathbf{b}}}\big\{-\lambda^k\,\mathbf{L}(\mathbf{a},\,\lambda^k)\big\}\,\big\{-1\,\big\}\,\big\{+\lambda^k\,\mathbf{L}(\mathbf{b},\,\lambda^k)\big\}\right] &(30)\\
&=\,\lim_{n\,\rightarrow\,\infty}\left[\frac{1}{n}\sum_{k\,=\,1}^{n}\,\lim_{\substack{\mathbf{s}_1\,\rightarrow\,\mathbf{a}\\ \mathbf{s}_2\,\rightarrow\,\mathbf{b}}}\Big\{+\,\big(\lambda^k\big)^2\,\mathbf{L}(\mathbf{a},\,\lambda^k)\;\mathbf{L}(\mathbf{b},\,\lambda^k)\Big\}\right] &(31)\\
&=\,\lim_{n\,\rightarrow\,\infty}\left[\frac{1}{n}\sum_{k\,=\,1}^{n}\,\mathbf{L}(\mathbf{a},\,\lambda^k)\,\mathbf{L}(\mathbf{b},\,\lambda^k)\right] &(32)\\
&=\,-\,\mathbf{a}\cdot\mathbf{b}\,-\,\lim_{n\,\rightarrow\,\infty}\left[\frac{1}{n}\sum_{k\,=\,1}^{n}\,\mathbf{L}(\mathbf{a}\times\mathbf{b},\,\lambda^k)\right] &(33)\\
&=\,-\,\mathbf{a}\cdot\mathbf{b}\,-\,\lim_{n\,\rightarrow\,\infty}\left[\frac{1}{n}\sum_{k\,=\,1}^{n}\,\lambda^k\right]\mathbf{D}(\mathbf{a}\times\mathbf{b}) &(34)\\
&=\,-\,\mathbf{a}\cdot\mathbf{b}\,+\,0\,. &(35)
\end{aligned}$$

Here Eq. (28) follows from Eq. (27) by substituting the functions $sign(+\,\mathbf{s}_1^k\cdot\mathbf{a})$ and $sign(-\,\mathbf{s}_2^k\cdot\mathbf{b})$ from the definitions (14) and (15); Eq. (29) follows from Eq. (28) by using the "product of limits equal to limits of product" rule [which can be verified by recognizing that the same quaternion $-\,\mathbf{D}(\mathbf{a})\,\mathbf{L}(\mathbf{a},\,\lambda^k)\,\mathbf{L}(\mathbf{b},\,\lambda^k)\,\mathbf{D}(\mathbf{b})$ results from the limits in Eqs. (28) and (29)]; Eq. (30) follows from Eq. (29) by (i) using the relation (16) [thus setting all bivectors in the spin bases], (ii) the associativity of the geometric product, and (iii) the conservation of spin angular momentum captured in Eq. (26); Eq. (31) follows from Eq. (30) by recalling that scalars such as λ^k commute with the bivectors; Eq. (32) follows from Eq. (31) by using $\lambda^2=+1$ and removing the superfluous limit operations; Eq. (33) follows from Eq. (32) by using the geometric product or identity (11), together with the fact that there is no third spin about the orthogonal direction $\mathbf{a}\times\mathbf{b}$ once the two spins are already detected along the directions $\mathbf{a}$ and $\mathbf{b}$; Eq. (34) follows from Eq. (33) by using the relations (16) and summing over the counterfactual detections of the "third" spins about $\mathbf{a}\times\mathbf{b}$; and Eq. (35) follows from Eq. (34) because the scalar coefficient of the bivector $\mathbf{D}(\mathbf{a}\times\mathbf{b})$ vanishes in $n\rightarrow\infty$ limit, since λ^k is a fair coin.

Note that, apart from the initial state λ^k, the only other assumption used in this derivation is that of the conservation of spin angular momentum (26). These two assumptions are necessary and sufficient to dictate the singlet correlations:

$$\mathcal{E}(\mathbf{a},\,\mathbf{b})\,=\,\lim_{n\,\rightarrow\,\infty}\left[\frac{1}{n}\sum_{k\,=\,1}^{n}\,sign(+\,\mathbf{s}_1^k\cdot\mathbf{a})\;sign(-\,\mathbf{s}_2^k\cdot\mathbf{b})\right]\,=\,-\,\mathbf{a}\cdot\mathbf{b}\,. \tag{36}$$

This demonstrates that EPR-Bell type correlations are correlations among the scalar points of a quaternionic 3-sphere. Given this result, it is not difficult to derive the corresponding upper bound on the expectation values within S^3 [1][4]:

$$|\,\mathcal{E}(\mathbf{a},\,\mathbf{b})\,+\,\mathcal{E}(\mathbf{a},\,\mathbf{b}')\,+\,\mathcal{E}(\mathbf{a}',\,\mathbf{b})\,-\,\mathcal{E}(\mathbf{a}',\,\mathbf{b}')\,|\,\leqslant\,2\sqrt{2}\,. \tag{37}$$

We have verified both of the above results in several numerical simulations [6][7][8][9]. The simulations are instructive on their own right and can be used for testing the effects of topology changes when a distributive parameter is varied.

Let us now turn to the practical problem of determining the direction of rotation of a bomb fragment. In order to minimize the contributions of precession and nutation about the rotation axis of the fragment, the bomb may be composed of two flexible squashy balls instead of a single ball. The two balls can then be squeezed together at the start of a run and released as if they were two parts of the same bomb. This will retain the spherical symmetry of the two constituent balls after the explosion, reducing their precession and nutation effects considerably. Consequently, we assume that during the narrow time window of the detection process the contributions of precession and nutation are negligible. In other words, during this narrow time window the individual spins will remain confined to the plane perpendicular to the horizontal direction of the setup. This is because we will then have $\mathbf{s} = \mathbf{r} \times \mathbf{p}$, with $\mathbf{r}$ specifying the location of the massive lump in the constituent ball and $\mathbf{p}$ being the ball's linear momentum. We can now exploit these physical constraints to determine the direction of rotation of a constituent ball unambiguously, as follows.

Since only the directions of rotation are relevant for computing the correlation function (1), it would be sufficient for our purposes to determine only the direction of the vector $\mathbf{s}$ at each end of the setup. This can be accomplished by arranging three (or more) successive laser screens perpendicular to the horizontal path of the constituent balls, say about half a centimeter apart, and a few judiciously situated cameras around them. To facilitate the detection of the rotation of a ball as it passes through the screens, the surface of the balls can be decorated with distinctive marks, such as dots of different sizes and colors. Then, when a ball passes through the screens, the entry points of a specific mark on the ball can be recorded by the system of cameras. Since the ball would be spinning while passing through the screens, the entry points of the same mark on the successive screens would be located at different relative positions on the screens. The rotation axis of the ball can therefore be determined unambiguously by determining the plane spanned by the entry points and the right-hand rule. In other words, the rotation axis can be determined as the orthogonal direction to the plane spanned by the entry points, with the sense of rotation determined by the right-hand rule. This procedure of determining the direction of rotation can be followed through manually, or it can be automated with the help of a computer software. Finally, the horizontal distance from the center of the setup to the location of the middle of the screens can be taken as the distance of the rotation axis from the center of the setup. This distance would help in establishing the simultaneity of the spin measurements at the two ends of the setup.

Undoubtedly, there would be many sources of errors in a mechanical experiment such as this one. If it is performed carefully enough, however, then the discussion above strongly suggests that it will unequivocally refute the prediction

$$\mathcal{E}(\mathbf{a},\,\mathbf{b}) \,=\, \begin{cases} -\,1\,+\,\frac{2}{\pi}\,\cos^{-1}(\mathbf{a}\cdot\mathbf{b}) & \text{if} \quad 0 \leq \cos^{-1}(\mathbf{a}\cdot\mathbf{b}) \leq \pi \\ \\ +\,3\,-\,\frac{2}{\pi}\,\cos^{-1}(\mathbf{a}\cdot\mathbf{b}) & \text{if} \quad \pi \leq \cos^{-1}(\mathbf{a}\cdot\mathbf{b}) \leq 2\pi\,, \end{cases} \tag{38}$$

which is based on an incorrect calculation by Bell [2] and Peres [3], and vindicate the refined prediction derived above,

$$\mathcal{E}(\mathbf{a},\,\mathbf{b}) = \lim_{n\,\gg\,1}\left[\frac{1}{n}\sum_{k\,=\,1}^{n}\left\{sign\,(\,+\,\mathbf{s}_1^k\cdot\mathbf{a})\right\}\left\{sign\,(\,-\,\mathbf{s}_2^k\cdot\mathbf{b})\right\}\right] \,=\, -\,\mathbf{a}\cdot\mathbf{b}\,, \tag{39}$$

which is based on the correct geometry and topology of the physical space, namely those of a quaternionic 3-sphere.

Acknowledgments

I wish to thank Fred Diether, Michel Fodje, Chantal Roth, and Albert Jan Wonnink for discussions and computing.

[1] J. Christian, Int. J. Theor. Phys. **54**, 2042 (2015); DOI:10.1007/s10773-014-2412-2; See also arXiv:1501.03393 (2015).
[2] J. S. Bell, Physics 1, 195 (1964); See also J. Christian, arXiv:0806.3078 (2008) and arXiv:1301.1653 (2013).
[3] A. Peres, Quantum Theory: Concepts and Methods (Kluwer, Dordrecht, 1993), p 161.
[4] J. Christian, *Disproof of Bell's Theorem: Illuminating the Illusion of Entanglement*, Second Edition (Brwonwalker Press, Boca Raton, Florida, 2014); See also arXiv:1106.0748 (2011), arXiv:1211.0784 (2012), and arXiv:1405.2355 (2014).
[5] C. Doran and A. Lasenby, *Geometric Algebra for Physicists* (Cambridge University Press, Cambridge, 2003).
[6] J. Christian, *A numerical simulation of the S^3 model for the EPR-Bohm correlation*, `http://rpubs.com/jjc/13965` (2014).
[7] J. Christian, *A 3-dimensional simulation of the 3-sphere model for the EPR-Bohm correlation*, `http://rpubs.com/jjc/84238` (2015) [see also `http://rpubs.com/jjc/99993` and `http://rpubs.com/jjc/105450`].
[8] A-J. Wonnink, `http://challengingbell.blogspot.co.uk/2015/03/numerical-validation-of-vanishing-of_30.html`, & C. F. Diether III, `http://challengingbell.blogspot.co.uk/2015/05/further-numerical-validation-of-joy.html`; See also C. F. Diether III, `http://www.sciphysicsforums.com/spfbb1/viewtopic.php?f=6&t=200&p=5550#p5514`.
[9] L. Dorst, D. Fontijne, and S. Mann, `http://geometricalgebra.org/gaviewer_download.html`.